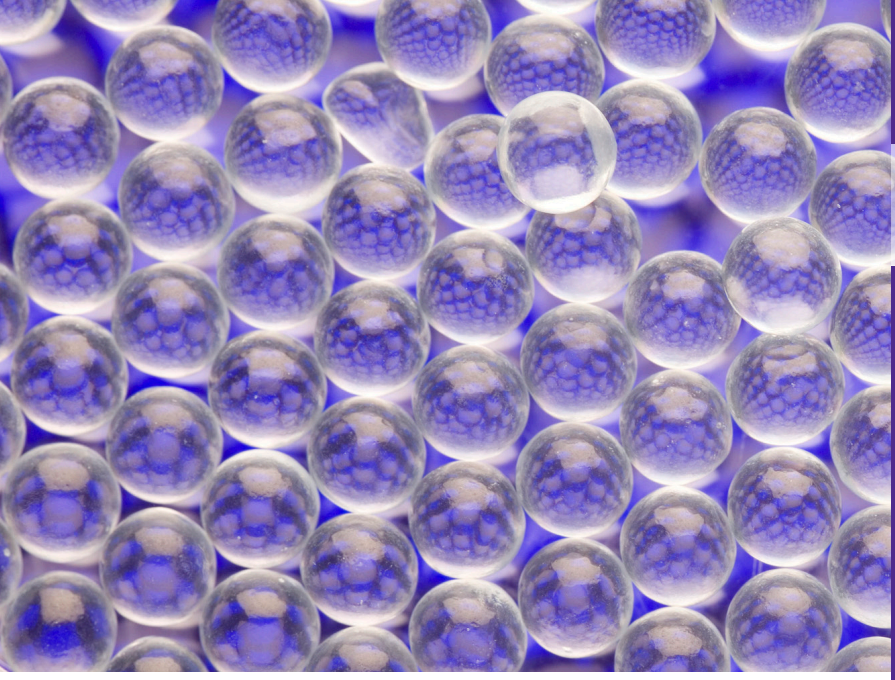

APPLICATION NOTE

ICP - Mass Spectrometry

AUTHORS

Ruth C. Merrifield

Jamie R. Lead

Center for Environmental NanoScience and Risk (CENR), Arnold School of Public Health
University of South Carolina, SC

Chady Stephan

PerkinElmer, Inc.
Shelton, CT

SP-ICP-MS Analysis of Size and Number Concentration in Mixtures of Monometallic and Bimetallic (Core-shell) Nanoparticles

Introduction

It is challenging to separate and measure the physical and chemical properties of monometallic and bimetallic engineered nanoparticles (NPs), especially when mixtures of NPs consist of particles of similar size, composition, and especially when present at low concentrations. Fully characterizing suspensions of NPs usually requires a multimethod approach to yield the most reliable results[1,2]. This process becomes increasingly difficult for more complex bimetallic NPs used in some applications or for those that require a mixture of different NPs, since differentiating between NPs can be a slow and arduous task. There are a variety of techniques that have been used for the determination of particle diameter, composition, and particle number concentration (part. mL^{-1}) of engineered NPs, including dynamic light scattering (DLS), field flow fractionation (FFF), ultraviolet/visible spectroscopy (UV/Vis), multi-angle light scattering (MALS), and, more recently, single particle inductively coupled plasma mass spectrometry (SP-ICP-MS)[3]. All these techniques have their own strengths and weaknesses as well as measuring size and/or composition in different ways.

PerkinElmer®
For the Better

Both DLS and FFF measure the particles' hydrodynamic diameter; however, FFF has the advantage of separating particles on the basis of their hydrodynamic size, making it unbiased to particle size, unlike DLS. While FFF separates particles by size, it must be coupled to a detector, traditionally UV/Vis, MALS, DLS, or fluorescence, all light source techniques that lack the required sensitivity for environmental-type research. For that, FFF has been coupled to ICP-MS, a more sensitive detector, which allows for lower detection limits of metal-based engineered nanomaterials than the above-mentioned detectors[4]. However, when dealing with a mixture of monometallic and bimetallic particles, simulating a random environmental sample, all these detection techniques will suffer to provide the particle number concentration.

One of the most difficult properties to routinely measure in a NP suspension is particle number concentration[3,5], which can be measured directly using techniques like nanoparticle tracking analysis (NTA)[6] or by a complex, multimethod approach[7]. However, these techniques have limitations when dealing with mixtures of NPs, as they do not offer compositional information.

As a standalone technique, single particle ICP-MS (SP-ICP-MS) has emerged as the technique of choice for the detection of metallic NPs at environmental levels, providing particle size, size distribution, and particle number concentration all on particle per particle basis[8]. In this work, we demonstrate the use of SP-ICP-MS as a standalone technique to measure complex suspensions of NPs and discriminate between mixtures of monometallic gold (Au) and silver (Ag) NPs and bimetallic Au@Ag (core-shell) NPs, yielding particle-size and particle-number concentrations for each constituent.

Experimental

Field Flow Fractionation (FFF)

An Eclipse DualTech FFF separation system from Wyatt (Wyatt Technology, Santa Barbara, California, USA) was used and equipped with a 10 KDa polyethersulfone (PES) hollow fiber (diameter of 0.8 mm and length of 17 cm, purchased from Wyatt) which was used as a separation channel. A detector flow of 0.5 mL/min and focus flow of 0.2 mL/min were used to focus the particles in the channel. These conditions were allowed to reach equilibrium for 2 minutes before injecting the sample, and then focusing for 10 minutes. The particle elution followed by ramping the cross flow from 0.15-0.6 mL/min over a 10-minute period (the particles eluted between 0.1 and 0.6 mL/min cross flow). A 5-minute post elution with no cross flow was used to clear the channel of any residual particles, resulting in a total analysis time of 27 minutes. Injection volumes of 2-20 µL were used. The carrier solution was 0.2 mM sodium citrate, and the separation was measured using a UV detector at 400 nm.

Inductively Coupled Plasma Mass Spectrometry (ICP-MS)

A PerkinElmer NexION® SP-ICP-MS equipped with Syngistix™ Nano Application software module, operating under the conditions outlined in Table 1, was used.

Table 1: NexION SP-ICP-MS Operating Conditions.

Parameter	Value
Nebulizer	MEINHARD®
Spray Chamber	Cyclonic
Power (W)	1600
Plasma Gas (L/min)	16
Aux Gas (L/min)	1.2
Neb Gas (L/min)	1.12
Sample Flow Rate (mL/min)	0.5 – 1
Dwell Time (µs)	50
Sampling Time (s)	60

Nanoparticles (NPs)

NP suspensions for this study were purchased from nanoComposix™ (San Diego, California, USA) and the National Institute of Standards Technology (NIST, Gaithersburg, Maryland, USA).

The following particles were used for this study: Ag 60 nm, Au 60 nm, Au@Ag 60 nm (Au core size 30 nm, Ag shell thickness 15 nm), Ag 80 nm, Au 80 nm, and Au@Ag 80 nm (Au core size 50 nm, Ag shell thickness 15 nm). The particle concentrations provided by the manufacturer are shown in Figure 1B and were diluted to between 10,000 and 100,000 particles (part.) mL^{-1} for SP-ICP-MS analysis, based on the manufacturers' data. For FFF analysis, the particles were used at the nominal concentrations of the stocks (Figure 1B) or diluted to 1,000,000 part. mL^{-1}, depending on injection volume used.

Standards

For SP-ICP-MS work, ionic Au and Ag standards at 1, 2, 3, and 4 ppb were used as ionic calibrations and made from 1000 mg/L stock standards. NIST Au NP standards of 30 nm and 60 nm were used for Au particle calibrations at concentrations of 100,000 part. mL^{-1}. The NIST 60 nm Au particles were used to determine the transport efficiency of the system.

Results and Discussion

NIST 30 and 60 nm certified reference materials (CRMs) were used to quantify the accuracy of the SP-ICP-MS measurements. The certified diameter and size distribution measured by TEM for the nominally 30 and 60 nm standards are 27.6 (± 2.1) and 56.3 (± 1.5) nm, respectively. Diameters of the same NPs measured by SP-ICP-MS are 26.9 (± 0.3) nm and 57.3 (± 0.1) nm, which is in excellent agreement with the certified values. Additionally, the measured particle number concentrations of the CRMs were within 3% of the certified values, validating the accuracy of SP-ICP-MS.

With the accuracy of SP-ICP-MS established, six test NP suspensions purchased from commercial sources (details shown in Table 2) were analyzed by SP-ICP-MS to determine particle size and concentration of each individual suspension for later reference. The commercial NPs have a higher degree of dispersity compared to the NIST reference standards, sometimes showing bimodal distributions, an example of which is shown in Figure 1A, where the Au 80 nm suspension has a peak at 60.4 (± 0.1) (dotted line) and at 78.1 (± 4.0) (dashed line). In addition, the commercial NPs showed an offset in particle number, an example of which is Ag 60 nm, showing a measured concentration that is 1.7 times lower than expected (Figure 1D). To simplify data analysis, we fitted a Gaussian curve to the size distributions (dotted-dashed line) and used these fits for data interpretation.

Figures 1B and 1C show the measured particle diameters and measured particle number concentrations for the individual NP suspensions, respectively. The total particle diameters for the separate Ag or Au NPs are 73.5 (3.9) nm, 76.2 (0.2) nm, 54.7 (0.2) nm, and 55.5 (0.3) nm for the nominally Au 80 nm, Ag 80 nm, Au 60 nm, and Ag 60 nm particles, respectively. The actual stated values from the manufacturers are 81.2 (10.5) nm, 78.9 (10.5) nm, 60.6 (5.9) nm, and 59.6 (5.8) nm, suggesting the information supplied by the manufacturer is accurate, but SP-ICP-MS is capable of greater precision. This supports the ability of SP-ICP-MS to easily identify bimodal distributions when they exist, as shown in Figure 1A.

SP-ICP-MS is a mass-based technique, thus particle size is determined from the total number of ions detected as individual particles. When analyzing core-shell structures, the converted size for silver in an Au@Ag 60 nm particle is 57.8 (± 0.3) nm and 74.3 (± 0.5) nm for an Au@Ag 80 nm particle. These calculated sizes can be directly compared to the manufacturer's (TEM) measurements of 60.8 (± 6.3) nm and 78.2 (± 8.8) nm. Figure 1C shows the particle number concentrations for each of the particle suspensions. All of the suspensions were diluted so that their concentration was expected to be 100,000 part. mL^{-1}.

Table 2: NP Suspensions Used in this Study.

Element	Description	Nominal Size (nm)
Ag	Pure Ag	60
	Pure Ag	80
Au	Pure Au	60
	Pure Au	80
Au@Ag	30 nm Au core, 15 nm Ag shell	60
	50 nm Au core, 15 nm Ag shell	80

It is evident that the manufacturer's data for most suspensions is accurate. However, the manufacturer's data for the Au 80 nm and Ag 60 nm were not in agreement with SP-ICP-MS, with the Au 80 nm sample containing significantly more particles and the Ag 60 nm sample containing significantly fewer particles than expected. Figure 1D compares the manufacturer's particle concentration with those measured by SP-ICP-MS, where the final column contains a correction factor which converts the accurate measured value to the manufacturer's value. As all samples were diluted per the manufacturer's data, this correction factor was applied to all measured particle numbers to make the analysis easier. For the core-shell NPs, the concentrations for both Ag and Au signals were identical, confirming that we do not have mixtures of Ag and Au samples.

Mixtures of Au@Ag, Au, and Ag NPs in SP-ICP-MS provide an extremely challenging test of the selectivity of SP-ICP-MS. Typical SP-ICP-MS data for mixtures of the 80 nm particles and 60 nm particles are shown in Figure 2. The Au and Ag signals for the 80 nm mixtures are shown in Figures 2A and 2B, respectively, and the Au and Ag signals for the 60 nm mixtures are shown in Figures 2C and 2D, respectively. The Gaussian fits for the single NP suspensions are shown. The dotted black lines represent the Gaussian fit for the monometallic NPs, while the dashed lines are for the bimetallic NPs. Figures 2A and 2C show a good separation of the signal from the Au core particles at 46.0 nm (A dashed line) and 29.5 nm (C dashed line), and the Au monometallic particles at 76.2 nm (A dotted line) and 54.7 nm (C dotted line). This separation allows the size and concentration of the core particles (from the Au@Ag NPs) to be differentiated from the monometallic Au NPs.

Figures 2B and 2D are the Ag signals for the 80 nm mixture and 60 nm mixture, respectively. In contrast to the Au signals, the Ag shell signal (dashed lines) and Ag monometallic NP (dotted lines) overlap, meaning they cannot be distinguished on the basis of SP-ICP-MS alone. (The peak separation needs to be twice the average of the full width half maxima of each peak to accurately measure size and particle number concentration counts).

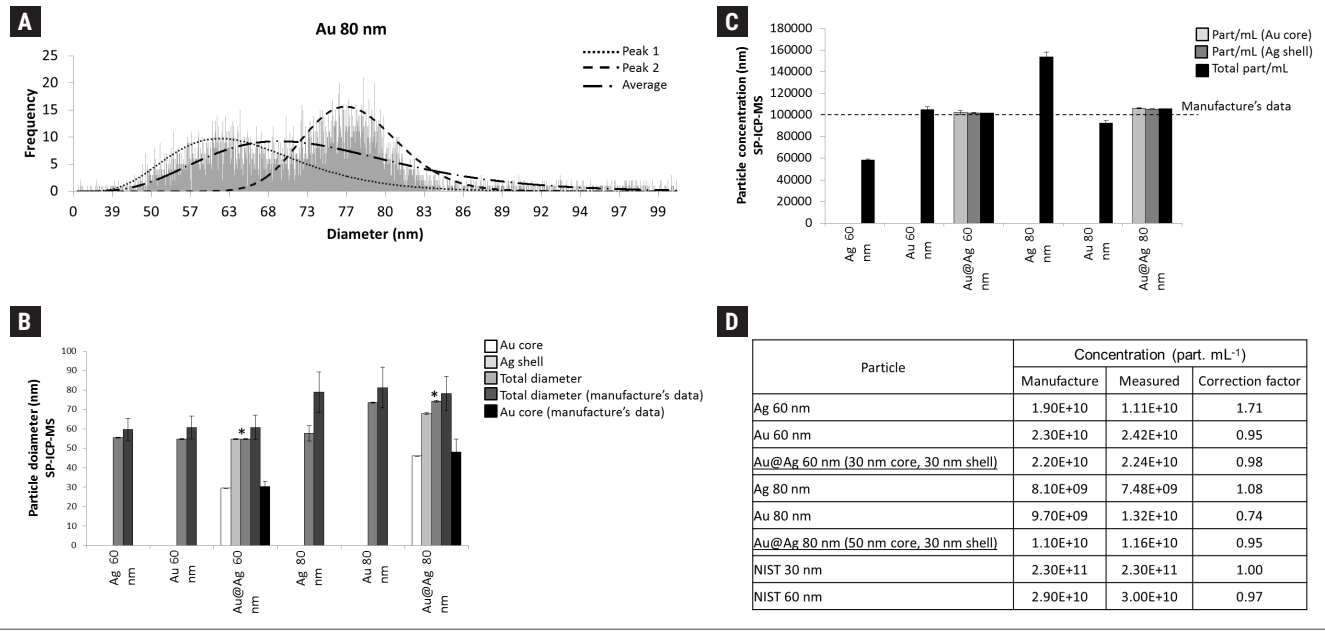

Particle	Concentration (part. mL^{-1})		
	Manufacture	Measured	Correction factor
Ag 60 nm	1.90E+10	1.11E+10	1.71
Au 60 nm	2.30E+10	2.42E+10	0.95
Au@Ag 60 nm (30 nm core, 30 nm shell)	2.20E+10	2.24E+10	0.98
Ag 80 nm	8.10E+09	7.48E+09	1.08
Au 80 nm	9.70E+09	1.32E+10	0.74
Au@Ag 80 nm (50 nm core, 30 nm shell)	1.10E+10	1.16E+10	0.95
NIST 30 nm	2.30E+11	2.30E+11	1.00
NIST 60 nm	2.90E+10	3.00E+10	0.97

Figure 1: A) Bimodal distribution measured for Au 80 nm NP suspension; B) and C) Particle diameters (B) and concentrations (C) for six nanoparticles; and D) Measured versus nominal concentrations of the particles along with the correction factor, as measured by SP-ICP-MS. All particle suspensions were diluted to 100,000 part. mL^{-1} based on the data provided by the manufacturer. The 'total diameter' is SP-ICP-MS data collected in this study, accounting for the core-shell geometry. Manufacturer's data is from transmission electron microscopy, although no data on sample preparation was provided. Figure 1D shows the measured particle numbers from SP-ICP-MS.

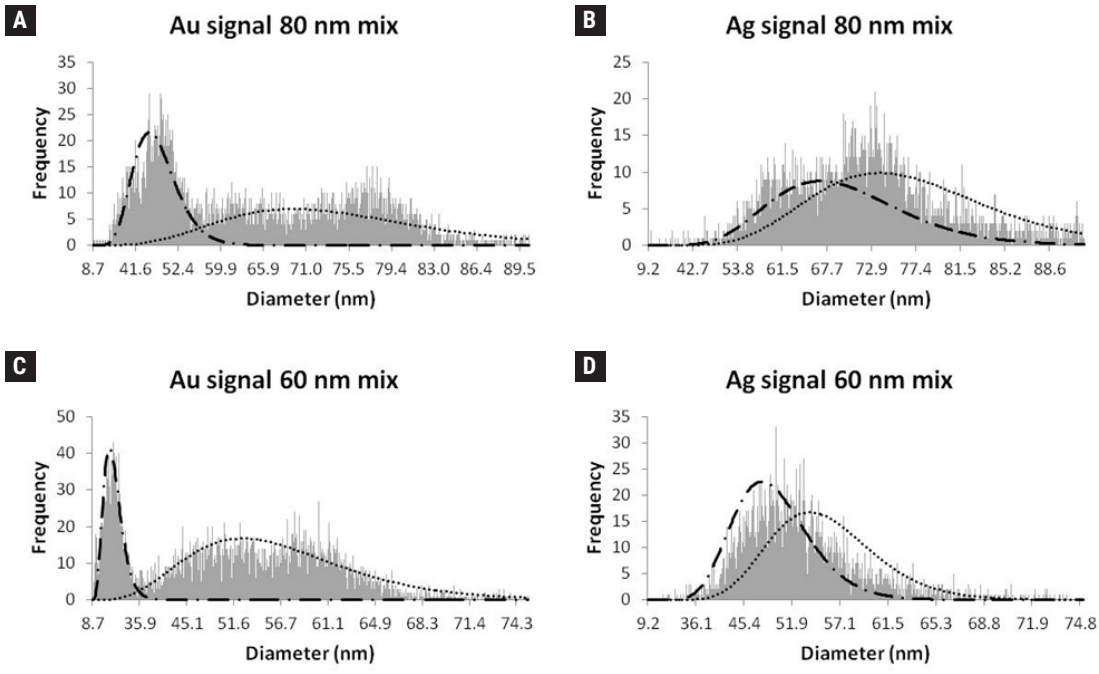

Figure 2: SP-ICP-MS particle size distribution for (A) Au from a mixture of 80 nm Au and 80 nm Au@Ag particles; (B) Ag from a mixture of 80 nm Ag and 80 nm Au@Ag particles; (C) Au from a mixture of 60 nm Au and 60 nm Au@Ag particles; (D) Ag from a mixture of 60 nm Ag and 60 nm Au@Ag particles The dotted black curve corresponds to the expected signal from the monometallic particles, and the dashed black curve shows the Gaussian curve from the bimetallic (core-shell) particles.

There is enough separation in the Au signal to determine the particle number concentration for both the Au monometallic particle and the Au core from the bimetallic NP. Despite the lack of separation in the Ag signal, it is still possible to calculate the particle number concentrations for all three NPs in the suspension. The Ag signal contains the particle numbers for both the Ag monometallic and Ag shell (from the Au@Ag NP). Since we know the particle number of the bimetallic NPs from the Au signal, we can subtract this from the total Ag signal to obtain a particle number concentration for the Ag monometallic NP. Thus, it is possible to calculate the concentrations of all the NPs.

Subsequent to this initial analysis, five mixtures of these NP suspensions were produced (Table 3). The particle diameters and particle number concentrations for the three mixtures containing Au 80 nm and Au@Ag 80 nm NPs (mixtures 1-3, Table 3) are shown in Figures 3A and 3B, respectively. For these samples, the Au signal contained information for both the Au core and Au monometallic NPs, while the Ag signal only contained information from the Ag shell. The total measured particle number concentration was used as a check to ensure that the particles were not being over- or under-represented. In all three mixtures, the total number of particles per mL measured for the Au signal is within 0.5% of the particles per mL measured for the smaller and larger peak combined. This means that all particles are only counted once, verifying that the methodology is truly a single particle analysis at these concentrations.

Table 3: Mixtures of Particles.

Mixture	Concentration (part. mL^{-1})		
	Au	Ag	Au@Ag
1. Au 80 and Au@Ag 80	80,000	-	20,000
2. Au 80 and Au@Ag 80	50,000	-	50,000
3. Au 80 and Au@Ag 80	20,000	-	80,000
4. Au 80, Ag 80, and Au@Ag 80	64,600	53,900	73,000
5. Au 60, Ag 60, and Au@Ag 60	100,000	66,000	40,000

Figure 3 shows that in all three mixtures of the Au and Au@Ag NPs, the correct particle sizes can be measured despite the relative mixture composition, and the particle number concentration changes with mixture composition in the expected manner. The total number of Au particles in each mixture is between 5 and 16% of the amount expected. In Figure 3A, the particle diameters for the Au 80 nm, Au-core, and Ag shell were all measured within 3% of those measured for the individual NPs. The particle number concentrations of the mixtures were not significantly different from their expected values, based on Figures 1 and 2, and the mixture ratios used. The challenge in back calculating the true individual values from a mixture becomes more pronounced where the mixture ratios are high (or low) and where the NP samples are polydisperse. For these bimodal suspensions and at these mixture ratios, the actual and expected values are in good agreement, with < 20% difference in size and number concentration. However, criteria must be worked out on a case by case basis.

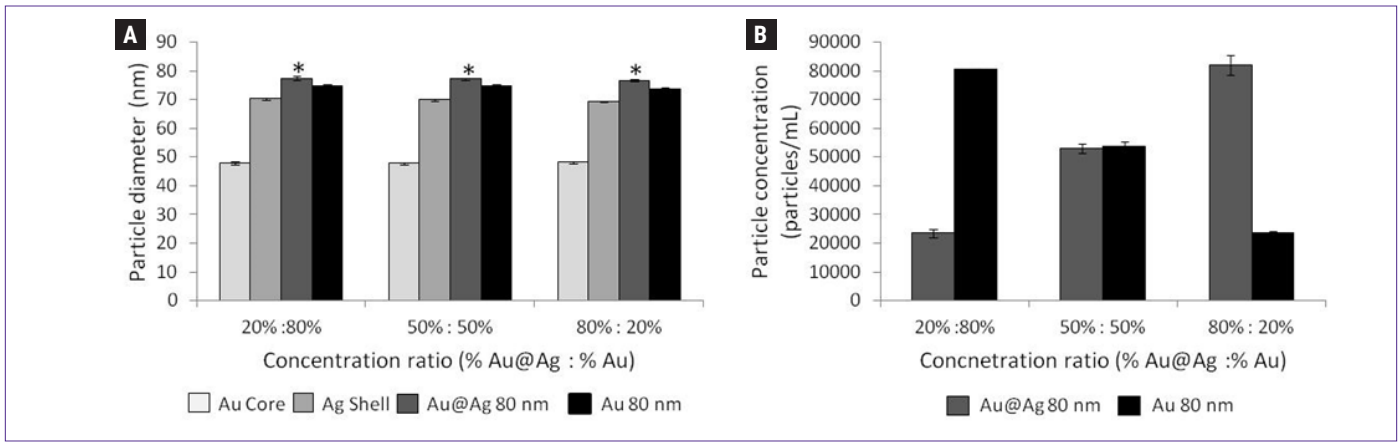

*Figure 3: Particle diameters (A) and particle number concentrations (B) for three particle suspensions as measured using SP-ICP-MS. All three suspensions contain Au@Ag 80 nm and Au 80 nm particles with different ratios of particle number concentrations: 1:4 (20,000:80,000), 1:1 (50,000:50,000) and 4:1 (80,000:20,000) part/mL (Au@Ag:Au).The total particle diameter for the Au@Ag 80 nm particle was calculated from the measured Au and Ag signal and is marked with an *.*

Figure 4 shows the measured sizes (Figure 4A) and calculated particle numbers (Figure 4B) for the 80 nm and 60 nm mixed NP suspensions of a three-component mixture of the Ag, Au and Au@Ag NPs. The Au core and NP can be quantitatively resolved due to their differences in size (Figures 2A and 2C), while the Ag signal cannot be resolved (Figures 2B and 2D). The Ag monometallic NPs and the Ag shell of the Au@Ag NPs are too similar to be resolved, so neither the Ag-monometallic NPs nor the total diameter for the Au@Ag NPs could be distinguished and calculated.

However, the particle number concentrations for all three particles are shown in Figure 4B. These were calculated from the acquired data, where the number of monometallic Au NPs are contained in the large peak of the Au signal (dashed line Figures 2A and 2C), the number of Au@Ag NPs can be found from the number of particles contained in the smaller peak (dotted line, Figure 2A and 2C), and the Ag signal contains the number of particles for both the Au monometallic and Au@Ag bimetallic NP combined, the latter of which can be removed from the Ag signal by subtracting the number measured for the small peak in the Au signal. The measured particle number concentrations for the 80 nm mixture are shown on the left-hand side of the graphs in Figure 4B. The particle number concentrations for the 80 nm mixture were approximately 66,100, 53,400, and 70,000 part. mL^{-1} for the Au, Ag, and Au@Ag particles, respectively. These particle number concentrations are within 5% of the original added amounts (64,600, 53,900, and 73,300 part. mL^{-1}), showing excellent agreement. For the nominally 60 nm particles, concentrations were within 7% of the expected values (107,000, 65,800, 37,800 part. mL^{-1} for the Au 60 nm, Ag 60 nm, and Au@Ag 60 nm particles compared to the expected values of 100,000, 66,000, and 40,000 part. mL^{-1}).

Data from a FFF with a UV detector was collected to show that the components of the 80 nm mixtures were eluting at the same time, confirming that the solution does indeed contain NPs of nominally the same diameter with no smaller particles present in the suspension. In this case, FFF cannot differentiate between monometallic Au or Ag or a bimetallic NP consisting of both Au and Ag. Figure 5 shows the elution of Au 80 nm, Ag 80 nm, Au@Ag 80 nm, and a mixture of all three compared to 40 and 80 nm polystyrene beads. A clear separation of the 40 and 80 nm polystyrene beads is visible, marked as features A (also shown in insert) and B in Figure 5, respectively. The 80 nm polystyrene beads and all the 80 nm metal particles elute close together, marked by features C and D in Figure 5. This shows that the Au@Ag particles and the Au 80 nm particles are of the same size. It is impossible to identify from the UV data if there are core-shell and solid metallic particles present in the suspension.

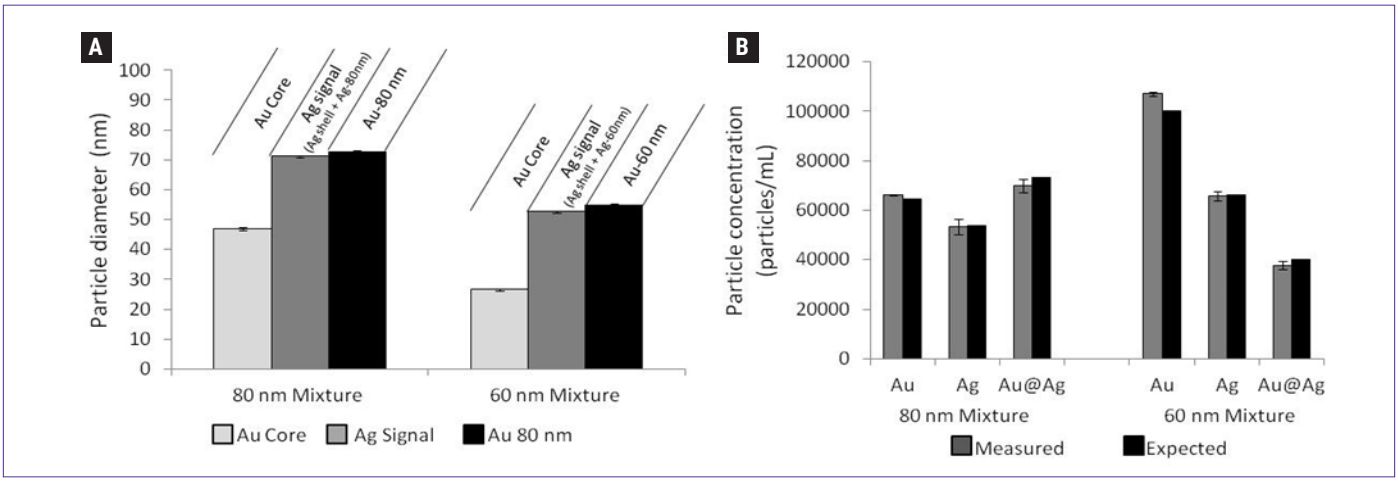

Figure 4: Particle diameters (A) and particle number concentrations (B) for two particle suspensions, as measured using SP-ICP-MS. The first suspension, an 80 nm mixture, contains Au 80 nm, Ag 80 nm and Au@Ag 80 nm NPs; the second mixture contains Au 60 nm, Ag 60 nm and Au@Ag 60 nm NPs. In (A) the diameters of the Au monometallic particles and the Au core from the Au@Ag NPs can be measured accurately, but the Ag signals from the monometallic and bimetallic particles are too close to resolve which signal belongs to which particle. However, from the data collected, all particle numbers can be calculated and can be seen to be close to the expected values in Figure 4B.

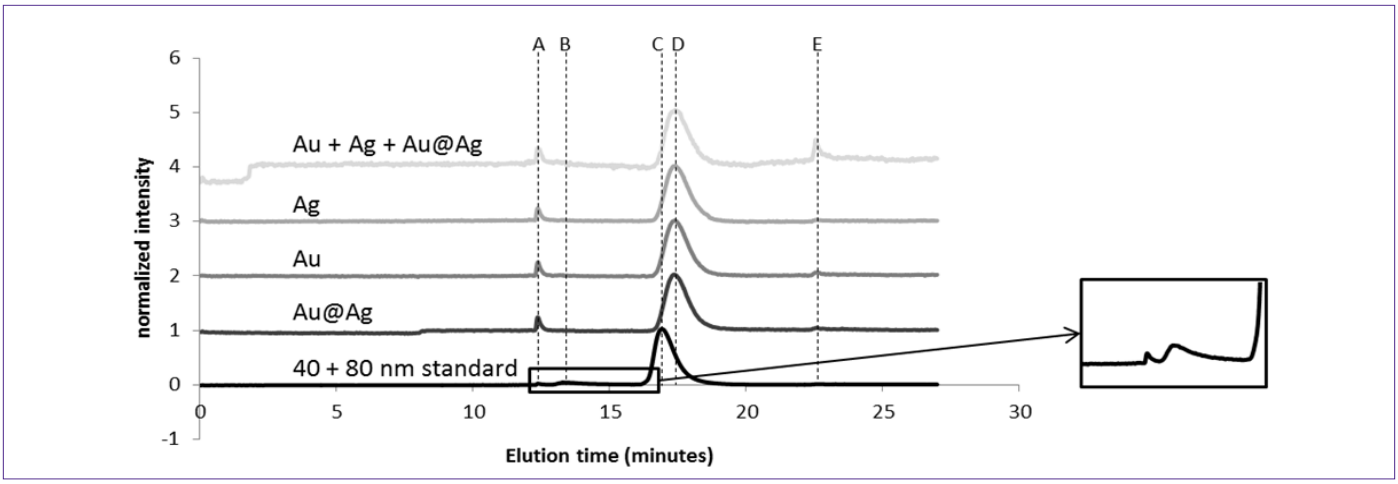

Figure 5: Fractograms showing elution of a mixture of 40 and 80 nm polystyrene beads, a solution of 80 nm Au@Ag NPs, 80 nm Au NPs, 80 nm Ag NPs, and a mixture of 80 nm Au+Ag+Au@Ag NPs, measured with a UV detector at a wavelength of 400 nm. The insert shows feature B associated with the 40 nm polystyrene beads.

Conclusion

This study has shown that PerkinElmer's NexION SP-ICP-MS is capable of collecting separate data on size and number concentration of complex mixtures of single metal and core-shell metal NPs while also being able to distinguish monometallic from bimetallic particles of the same size. The obtained data resolution shows that this method is an excellent addition to a multi-method approach[9] for NP metrology in complex systems, offering a greater level of precision when it relates to particle number and size distribution.

References

1. Baalousha, M.; Ju-Nam, Y.; Cole, P. A.; Gaiser, B.; Fernandes, T. F.; Hriljac, J. A.; Jepson, M. A.; Stone, V.; Tyler, C. R.; Lead, J. R., Characterization of cerium oxide nanoparticles-Part 1: Size measurements. Environmental Toxicology and Chemistry 2012, 31, (5), 983-993.

2. Baalousha, M.; Ju-Nam, Y.; Cole, P. A.; Hriljac, J. A.; Jones, I. P.; Tyler, C. R.; Stone, V.; Fernandes, T. F.; Jepson, M. A.; Lead, J. R., Characterization of cerium oxide nanoparticles-Part 2: Nonsize measurements. Environmental Toxicology and Chemistry 2012, 31, (5), 994-1003.

3. Shang, J.; Gao, X., Nanoparticle counting: towards accurate determination of the molar concentration. Chemical Society Reviews 2014, 43, (21), 7267-7278.

4. Mitrano, D. M.; Barber, A.; Bednar, A.; Westerhoff, P.; Higgins, C. P.; Ranville, J. F., Silver nanoparticle characterization using single particle ICP-MS (SP-ICP-MS) and asymmetrical flow field flow fractionation ICP-MS (AF4-ICP-MS). Journal of Analytical Atomic Spectrometry 2012, 27, (7), 1131-1142.

5. Li, M.; Guha, S.; Zangmeister, R.; Tarlov, M. J.; Zachariah, M. R., Method for Determining the Absolute Number Concentration of Nanoparticles from Electrospray Sources. Langmuir 2011, 27, (24), 14732-14739.

6. Malloy, A., Count, size and visualize nanoparticles. Materials Today 2011, 14, (4), 170-173.

7. Baalousha, M.; Sikder, M.; Prasad, A.; Lead, J.; Merrifield, R.; Chandler, G. T., The concentration-dependent behaviour of nanoparticles. Environmental Chemistry 2016, 13, (1), 1-3.

8. Laborda, F.; Jimenez-Lamana, J.; Bolea, E.; Castillo, J. R., Critical considerations for the determination of nanoparticle number concentrations, size and number size distributions by single particle ICP-MS. Journal of Analytical Atomic Spectrometry 2013, 28, (8), 1220-1232.

9. Domingos, R. F.; Baalousha, M. A.; Ju-Nam, Y.; Reid, M. M.; Tufenkji, N.; Lead, J. R.; Leppard, G. G.; Wilkinson, K. J., Characterizing Manufactured Nanoparticles in the Environment: Multimethod Determination of Particle Sizes. Environmental Science & Technology 2009, 43, (19), 7277-7284.

Consumables Used

Component	Description	Part Number
Sample Uptake Tubing	Green/orange (0.38 mm id) flared PVC	N0777042
Drain Tubing	Grey/grey (1.30 mm id) Santoprene	N0777444
Gold Standard	1000 mg/L aqueous gold standard, 125 mL	N9303759
Silver Standard	1000 mg/L aqueous silver standard, 125 mL	N9300171

Though detection limits, background equivalent concentrations and sensitivities may vary, the method presented in this work (e.g. isotope selection, gas choice, sample intro materials and properties etc.) is transferable to any PerkinElmer NexION ICP-MS system which can match the cell gas and analyzer quadrupole requirements.

PerkinElmer, Inc.
940 Winter Street
Waltham, MA 02451 USA
P: (800) 762-4000 or
(+1) 203-925-4602
www.perkinelmer.com

844612 (012821_01) PKI